

Ionization Energies and Dyson Orbitals of 1,2-Dithiin

J. V. Ortiz*

Department of Chemistry, Kansas State University, Manhattan, Kansas 66506-3701

Received: February 26, 2002; In Final Form: April 16, 2002

Photoelectron spectra of 1,2-dithiin are assigned with ab initio electron propagator calculations of vertical ionization energies and corresponding Dyson orbitals. Close agreement with experimental peaks obtains for the first nine final states. Dyson orbitals for the first three vertical ionization energies are composed chiefly of sulfur 3p and butadiene π fragment orbitals. Constructive interference between the second highest occupied π orbital of butadiene and sulfur 3p orbitals is seen in the Dyson orbitals pertaining to the fourth and seventh ionization energies. Weak σ bonding between sulfur atoms is found in the Dyson orbital for the fifth final state.

Introduction

Sunflowers and related plants in the *Asteraceae* family contain 1,2-dithiin derivatives that fascinate medicinal and theoretical chemists alike. The former have demonstrated the extensive antiviral, antifungal, antibacterial, and nematocidal properties of thiarubrines A and B.¹ The syntheses of 1,2-dithiin pigments and the antibiotic activity of these compounds in darkness and in light have been widely investigated.^{2,3} Theoretical interest issues from the possible antiaromaticity of six-member, eight-electron rings, tautomerism pertaining to ring-opened forms, and the stability of variational ansätze.^{4–10} Configuration interaction calculations on the lowest excited states have provided explanations for the redness of 1,2-dithiin in terms of wave functions dominated by excited determinants where an electron is promoted from one of the highest occupied molecular orbitals of the ground state to the lowest unoccupied molecular orbital.^{4,11} Gas-phase, photoelectron spectra (PES) of 1,2-dichalcogenins¹¹ have been interpreted in terms of Hartree–Fock molecular orbitals and their energies.

In this paper, the PES of 1,2-dithiin are investigated with correlated, ab initio electron propagator methods.^{12–15} With these techniques, it is possible to systematically calculate correlation corrections to the results of Koopmans's theorem (KT), where energies of frozen, Hartree–Fock orbitals are used to estimate electron binding energies. Orbital relaxation in the final state and differences in electron correlation energy between the initial and final states are taken into account in the propagator calculations. To each ionization energy (IE) calculated with these methods, there corresponds a Dyson orbital, ψ^{Dyson} , that represents the overlap between the initial, N -electron state, Ψ_N , and the final state with $N-1$ electrons, Ψ_{N-1} . Dyson orbitals are defined by

$$\psi^{\text{Dyson}}(x_1) = \sqrt{N} \int \Psi_N(x_1, x_2, x_3, \dots, x_N) \times \Psi_{N-1}^*(x_2, x_3, x_4, \dots, x_N) dx_2 dx_3 dx_4, \dots, dx_N \quad (1)$$

where x_i is the space-spin coordinate of electron i . (Dyson orbitals are also known as Feynman–Dyson amplitudes; these concepts first arose in quantum field theory.) The norm of the

Dyson orbital is known as the pole strength, p , and is given by

$$p = \int |\psi^{\text{Dyson}}(x_1)|^2 dx_1 \quad (2)$$

such that

$$0 \leq p \leq 1 \quad (3)$$

Photoionization intensities are proportional to pole strengths and to squares of transition operator matrix elements between Dyson orbitals and continuum orbitals that describe the ejected electron. In the uncorrelated Koopmans picture, pole strengths equal unity and Dyson orbitals are equal to canonical, Hartree–Fock orbitals. Electron propagator calculations supersede Koopmans results by providing direct determinations of correlated IEs, Dyson orbitals, and pole strengths without evaluation of the many-electron wave functions of the initial or final states.

Methods

Geometry optimizations are performed with Gaussian 98.¹⁶ Electron propagator calculations are executed with a link connected to this program.

The NR2 electron propagator approximation¹⁷ is employed in tests of basis set effects on calculated vertical IEs. This method has been shown to provide accurate accounts of the outer valence PES of closed-shell molecules, with an average absolute error of approximately 0.15 eV when a basis set of triple ζ quality or better is employed. Given the unusual bonding and the multiconfigurational character that characterize the ground state 1,2-dithiin, one cannot expect similar accuracy from NR2 calculations here. Nonetheless, the computational efficiency and rough accuracy of the NR2 method make it suitable for evaluating basis set effects.

Basis sets for electron propagator calculations are constructed as follows. For sulfur, the McLean–Chandler (12s,9p/6s5p) contraction for anions¹⁸ is supplemented by d and f polarization functions with 0.5 and 0.55 exponents, respectively. For carbon and hydrogen, Dunning's (10s,6p/5s3p) and (5s/3s) contractions¹⁹ are used. Carbon d functions with 0.65 exponents and hydrogen p functions with 0.75 exponents are added.

Several augmentations to the (6s5p1d1f,5s3p1d,3s1p) basis were examined sequentially in NR2 IE calculations.

* To whom correspondence should be addressed. E-mail: ortiz@ksu.edu.

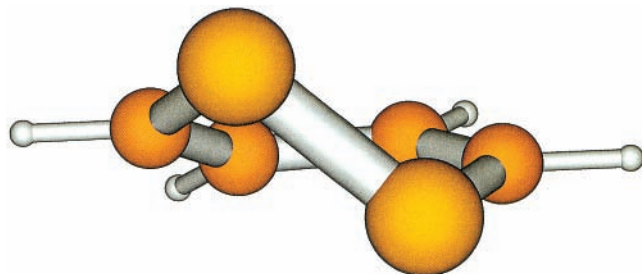


Figure 1. Structure of 1,2-dithiin.

1. Double sets of d or f polarization functions on sulfur and double sets of d polarization functions on carbon. (Double sets of polarization functions are derived by multiplying the original exponents by 0.5 and 2.0.)

2. Diffuse s and p functions on sulfur or carbon. (Multiplying the smallest s and p exponents by 0.3 defines diffuse function exponents.)

3. Carbon f (0.75 exponent) functions.

4. Sulfur g (0.683 exponent) functions.

In NR2 calculations on the first three final states, none of the augmentations in the first two categories increased the IE by more than 0.02 eV and some actually reduced the calculated electron binding energy. Carbon f and sulfur g functions increased the predicted IEs by approximately 0.03 and 0.04 eV, respectively.

Strong correlation effects in the ground state of 1,2-dithiin indicate the need for a reference state that is superior to the Hartree–Fock wave function used in NR2 calculations. The BD-T1 electron propagator approximation,¹⁵ which employs a Brueckner doubles, coupled-cluster reference state,^{20,21} is used, therefore. BD-T1 results on IEs of closed-shell molecules improve on NR2 values and are clearly superior for anion electron detachment energies,²² core IEs²³ and IEs of biradicaloid species such as ozone.²⁴ BD-T1 IEs therefore are calculated with the (6s5p1d1f,5s3p1d,3s1p) basis set.

Core orbitals are omitted from summations that are performed in the electron propagator calculations. IEs are converged to within 0.01 millihartrees.

Plots of the optimized geometry of 1,2-dithiin (Figure 1) and of Dyson orbitals produced by the (6s5p1d1f,5s3p2d,3s1p) basis (Fig.s 2 and 3) are made with MOLDEN.²⁵ Contours represent amplitudes of ± 0.075 .

Results and Discussion

Structure. The geometry of the 1,2-dithiin molecule was optimized with second-order, many-body perturbation theory²⁶ and the 6-311G(d,p) basis.^{18,27,28} The initial guess structure was taken from MP2/6-31+G(d) data in the PES report.¹¹ Optimization yields a structure that closely reproduces the experimental values based on microwave spectroscopy.²⁹ Table 1 shows these results. Relaxation of all symmetry constraints in the initial guess of ref 11 leads to a C_1 structure whose total energy agrees with that of the present C_2 structure to within 0.1 millihartree. Only the S–S bond length displays a significant disagreement with experiment. This discrepancy is remedied by adding f functions with 0.55 exponents from the sulfur 6-311G(df) basis.³⁰ A significantly shorter S–S separation results and all bond length errors are less than 0.004 Å. Figure 1 displays this structure, which is used in subsequent calculations of IEs.

Vertical Ionization Energies. IEs and pole strengths in several approximations are tabulated in Table 2. Irreducible representations of the C_2 point group label the final states. BD-T1 pole strengths lie between 0.85 and 0.90. When each of the

TABLE 1: 1,2-Dithiin Structure

parameter	MP2/6-311G(d,p)	MP2/6-311G(d,p) + S f	exptl ²⁹
S–S (Å)	2.082	2.051	2.051(3)
S–C	1.762	1.760	1.759(4)
C=C	1.355	1.355	1.353(3)
C–C	1.455	1.455	1.451(1)
S–S–C (°)	97.5	97.8	98.7(2)
S–C–C	122.1	121.6	121.4(2)
C–C–C	123.9	123.8	124.2(2)
S–S–C–C	-43.2	-43.5	-41.2
C–S–S–C	55.1	55.9	53.9
C–C–C–C	27.4	27.7	29.
C–C–C–S	2.3	2.0	0.3

TABLE 2: Ionization Energies (eV) and Pole Strengths

final state	PES ¹¹	BD-T1 p	NR2 ^a p	KT p
X ² A	8.16	8.01	7.92	8.32
		0.90	0.88	1.
A ² B	9.82	9.72	9.62	10.42
		0.89	0.87	1.
B ² A	10.06	9.78	9.72	10.38
		0.89	0.87	1.
² B			10.37	
			0.02	
C ² B	11.51	11.57	11.47	12.57
		0.88	0.80	1.
² B			11.98	
			0.02	
D ² A	12.17	12.20	12.01	13.03
		0.88	0.83	1.
² A			12.41	
			0.02	
E ² A	12.66	12.75	12.75	14.22
		0.88	0.83	1.
² A			12.98	
			0.05	
F ² B	13.15	13.02	12.58	14.42
		0.86	0.48	1.
² B			12.99	
			0.23	
² B			13.68	
			0.10	
G ² B	14.40	14.71		16.61
		0.85		1.
H ² A	14.97	14.93		16.82
		0.86		1.

^a NR2 produces spurious cationic states with low pole strengths (p) because of the inadequacy of the Hartree–Fock orbitals it employs.

Dyson orbitals is normalized to unity and expanded in terms of reference state orbitals, there is a dominant coefficient between 0.98 and 1.00 from a single, occupied Brueckner orbital. In contrast, corresponding NR2 pole strengths are often lower than 0.85 and corresponding Dyson orbitals have significant contributions from more than one canonical Hartree–Fock orbital. The occupied Brueckner orbitals and the Dyson orbitals for ionization energies are, in general, somewhat less diffuse than their occupied, Hartree–Fock counterparts. NR2 also yields many correlation final states with pole strengths that are less than 0.8. These results indicate that the Hartree–Fock reference state that is used in NR2 calculations is not always suitable for a description of the 1,2-dithiin photoelectron spectrum.

BD-T1 and NR2 calculations disagree with KT results on the order of the second and third final states. Discrepancies between calculated and experimental values are largest in the KT column and are smallest in the BD-T1 column. BD-T1 calculations with a basis set containing carbon f and sulfur g functions are not currently feasible, but these improvements are likely to improve agreement between theory and experiment for the first three IEs.

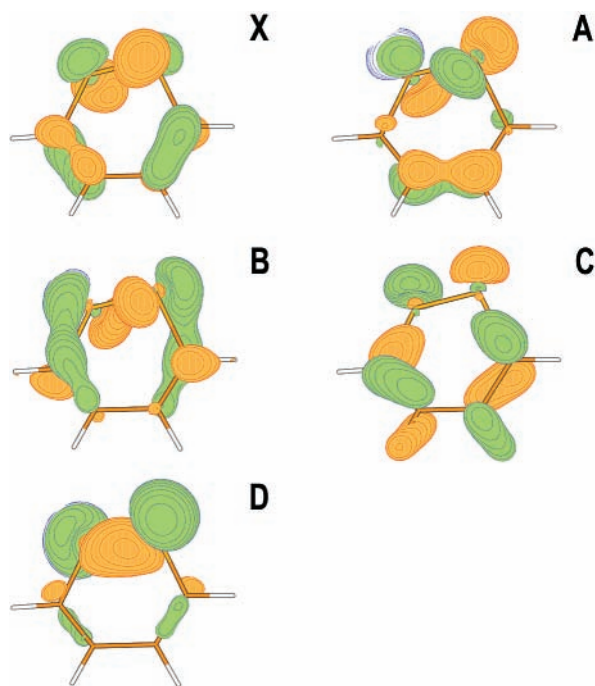


Figure 2. Dyson orbitals (correlated generalizations of occupied, Hartree–Fock orbitals) for IEs corresponding to the X^2A , A^2B , B^2A , C^2B , and D^2A cationic states of 1,2-dithiin.

Since the pole strength is close to 0.9 for the lowest IE and Dyson orbitals calculated in the NR2 and BD-T1 approximations are in close agreement, the Koopmans description is qualitatively valid for the X^2A final state. The corresponding Dyson orbital displays a combination of π lobes in the C_3 – C_4 and C_5 – C_6 internuclear regions that resembles the highest occupied orbital of butadiene, for there is a node in the C_4 – C_5 region. (See Figure 2.) All C–S and S–S interactions are π antibonding in this Dyson orbital. S–S π antibonding is only slightly reduced by a tilting of the sulfur 3p contributions. All of these interactions are reduced somewhat by the nonplanarity of the ring and the consequent lowering of symmetry from C_{2v} to C_2 . Minor sulfur 3s mixing allows the larger lobes of the resulting sulfur hybrid orbitals to point away from the neighboring sulfur lobes while the smaller lobes introduce some S–S σ bonding. Despite this accommodation, C–S and S–S π antibonding relationships predominate.

In the A^2B state, the largest contribution to the Dyson orbital is made by sulfur 3p orbitals that adopt perpendicular orientations to reduce S–S π antibonding. A π antibonding relationship also obtains between the S_2 fragment and the lobes of the other ring atoms, which now resemble the second highest occupied orbital of butadiene. Mixing from the butadiene π^* orbital decreases the C_3 and C_6 contributions relative to those from C_4 and C_5 , thus diminishing the C–S antibonding relationship. Despite the large discrepancy between the experimental IE and KT results, the pole strengths in the correlated calculations remain large and the correlated Dyson orbitals from NR2 and BD-T1 calculations strongly resemble the second highest occupied Hartree–Fock orbital. The Koopmans picture of this ionization therefore is qualitatively valid.

For the B^2A cation state, the pole strength and Dyson orbital results also qualitatively confirm the Koopmans picture. In contrast with the X^2A Dyson orbital, here there are bonding interactions between the C_4H_4 and S_2 fragments. These bonding relationships are accentuated by sulfur 3p orbitals that are oriented for C–S π bonding. This arrangement of sulfur 3p orbitals avoids S–S π antibonding and assists S–S σ bonding.

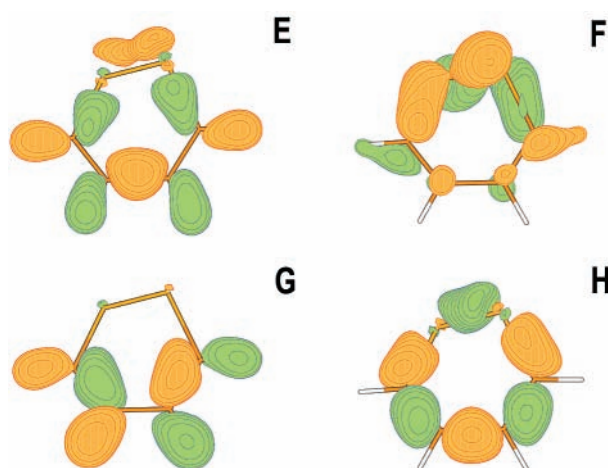


Figure 3. Dyson orbitals (correlated generalizations of occupied, Hartree–Fock orbitals) for IEs corresponding to the E^2A , F^2B , G^2B , and H^2A cationic states of 1,2-dithiin.

In comparison with the first two cases, carbon contributions are smaller in this Dyson orbital. Therefore, the interpretation of intensity changes from He I to He II spectra made in ref 11 is confirmed.

Differential correlation effects reverse the order of the second 2A and the first 2B states. These states are separated by approximately 0.1 eV and account for the enhanced area of the second peak relative to that of the first peak in the PES. A superior fit of the PES was obtained when two Gaussians were used for the second feature.¹¹

In the C^2B state, the Koopmans description retains its qualitative validity, but the Dyson orbital bears closer resemblance to an occupied Brueckner orbital than to the corresponding Hartree–Fock orbital. The pole strength is significantly larger in the BD-T1 calculation than in the NR2 result. Two spurious shake-up states with low pole strengths are predicted at the NR2 level. Despite these deficiencies, the NR2 IE is also in good agreement with experiment. Sulfur lone pair and a variety of two-center bonding lobes form a pattern of alternating phases in the Dyson orbital. The pattern in the butadiene sector is created by interference between the second highest occupied π orbital and σ orbitals of this fragment.

Strong σ bonding between the sulfurs is seen in the Dyson orbital for the D^2A state. Here two sulfur 3p orbitals tilt slightly away from the S–S axis and toward the interior of the ring. Lobes outside the ring are large. This nonbonding character accounts for the relative sharpness of the corresponding feature in the PES, for there are several other orbitals that contribute to S–S bonding. As in the previous case, the Dyson orbital more closely resembles an occupied Brueckner orbital than the corresponding Hartree–Fock orbital.

In the Dyson orbitals for the E^2A , G^2B , and H^2A final states, the dominant features are σ bonding lobes. (See Figure 3.) An in-plane, π interaction between the sulfurs may be seen in the E^2A Dyson orbital. A small S–S σ bonding contribution is present in the H^2A Dyson orbital, which features lobes with alternating phases in the ring.

S–S π bonding interactions are present in the Dyson orbital for the F^2B final state. There is some delocalization into lobes that resemble those of the second highest occupied π orbital of butadiene.

Pole strengths in BD-T1 calculations remain between 0.85 and 0.88 for the D^2A through H^2A final states. NR2 calculations produce considerably smaller pole strengths, especially in the case of the F^2B final state.

A simplified analysis of the Dyson orbitals may be based on two butadiene fragment π orbitals and S–S π bonding and antibonding orbitals. The highest occupied butadiene orbital mixes constructively or destructively with the S–S antibonding orbital in the X²A and B²A Dyson orbitals. In the latter case, however, the sulfur 3p orbitals tilt so that S–S π antibonding is avoided. Some S–S σ bonding also is induced in this way. In the A²B Dyson orbital, the lower butadiene π fragment orbital mixes with a combination of sulfur 3p orbitals that are nearly perpendicular. The S–S relationship thus is nonbonding. This butadiene fragment orbital also contributes to the Dyson orbitals of the F²B and the C²B final states.

Conclusions

In calculations of the vertical IEs of 1,2-dithiin, strong correlation effects in the ground state require the use of the Brueckner doubles reference state instead of a Hartree–Fock wave function. (Geometry optimizations are less sensitive to these correlation effects and the usual perturbative methods generate excellent bond lengths and angles.) For this reason, BD-T1 electron propagator calculations improve on NR2 IEs, pole strengths and Dyson orbitals. While NR2 calculations are in closer agreement with experiment than KT results for final states with high pole strengths, they produce many spurious correlation final states with low pole strengths.

The order of the first three final states is ²A, ²B, ²A in the correlated calculations, although the separation of the second and third states is less than 0.1 eV. This result accounts for the observation of a second peak with larger intensity in the PES.¹¹ Subsequent final states are ²B, ²A, ²A, ²B, ²B and ²A.

Dyson orbitals corresponding to the first three IEs represent mixtures of butadiene π and sulfur 3p orbitals. Carbon contributions to the third final state's Dyson orbital are larger than those for the first two final states' Dyson orbitals, in agreement with the interpretation of intensity changes from He I to He II spectra.¹¹

The Dyson orbital for the fifth final state is concentrated on the sulfurs and displays a weak σ bonding interaction. This result also confirms a clear trend in intensities when the ionizing source is changed from He I to He II.¹¹

Various combinations of σ bonding lobes occur in the Dyson orbitals of the sixth, eighth and ninth final states. S–S π bonding is found in the seventh final state's Dyson orbital.

Acknowledgment. This work was supported by the National Science Foundation under Grant CHE-9873897 and by the Petroleum Research Fund.

References and Notes

(1) Bierer, D. E.; Dener, J. M.; Dubenko, L. G.; Gerber, R. E.; Litvak, J.; Peterli, S.; Peterli-Roth, P.; Truong, T. V.; Mao, G.; Bauer, B. E. *J. Med. Chem.* **1995**, *38*, 2628.

(2) Block, E.; Birringer, M.; DeOrazio, R.; Fabian, J.; Glass, R. S.; Guo, C.; He, C.; Lorange, E.; Qian, Q.; Schroeder, T. B.; Shan, Z.; Thiruvazhi, M.; Wilson, G. S.; Zhang, X. *J. Am. Chem. Soc.* **2000**, *122*, 5052 and references therein.

(3) Block, E.; DeOrazio, R.; Guo, C.; Page, J.; Sheridan, R. S.; Toscano, J.; Towers, G. H. N. *J. Am. Chem. Soc.* **1996**, *118*, 4719.

(4) Cimiriaglia, R.; Fabian, J.; Hess, B. A. *J. Mol. Struct.* **1991**, *230*, 287.

(5) Mann, M.; Fabian, J. *J. Mol. Struct.* **1995**, *331*, 51.

(6) Pitchko, V.; Goddard, J. D. *Chem. Phys. Lett.* **1998**, *289*, 391.

(7) Ishida, T.; Oe, S.; Aihara, J. *J. Mol. Struct.* **1999**, *461–2*, 553.

(8) Aihara, J.; Ishida, T. *Bull. Chem. Soc. Jpn.* **1999**, *72*, 937.

(9) Orlova, G.; Goddard, J. D. *J. Chem. Phys.* **2000**, *112*, 10085.

(10) Fabian, J.; Mann, M.; Petiau, M. *J. Mol. Model.* **2000**, *6*, 177.

(11) Glass, R. S.; Gruhn, N. E.; Lichtenberger, D. L.; Lorange, E.; Pollard, J. R.; Birringer, M.; Block, E.; DeOrazio, R.; He, C.; Shan, Z.; Zhang, X. *J. Am. Chem. Soc.* **2000**, *122*, 5065. A preliminary report appeared in Glass, R. S.; Pollard, J. R.; Schroeder, T. B.; Lichtenberger, D. L.; Block, E.; DeOrazio, R.; Guo, C.; Thiruvazhi, M. *Phosphorus, Sulfur, Silicon* **1997**, *120–121*, 439.

(12) Linderberg, J.; Öhrn, Y. *Propagators in Quantum Chemistry*; Academic Press: New York, 1973.

(13) Ortiz, J. V. In *Computational Chemistry: Reviews of Current Trends*; Leszczynski, J., Ed.; World Scientific: Singapore, 1997; Vol. 2, p 1.

(14) Ortiz, J. V. In *Conceptual Perspectives in Quantum Chemistry*; Calais, J.-L.; Kryachko, E., Eds.; Kluwer: Dordrecht, 1997; Vol. 3, p 465.

(15) Ortiz, J. V. *Adv. Quantum Chem.* **1999**, *35*, 33.

(16) Frisch, M. J.; Trucks, G. W.; Schlegel, H. B.; Scuseria, G. E.; Robb, M. A.; Cheeseman, J. R.; Zakrzewski, V. G.; Montgomery, J. A., Jr.; Stratmann, R. E.; Burant, J. C.; Dapprich, S.; Millam, J. M.; Daniels, A. D.; Kudin, K. N.; Strain, M. C.; Farkas, O.; Tomasi, J.; Barone, V.; Cossi, M.; Cammi, R.; Mennucci, B.; Pomelli, C.; Adamo, C.; Clifford, S.; Ochterski, J.; Petersson, G. A.; Ayala, P. Y.; Cui, Q.; Morokuma, K.; Malick, D. K.; Rabuck, A. D.; Raghavachari, K.; Foresman, J. B.; Cioslowski, J.; Ortiz, J. V.; Stefanov, B. B.; Liu, G.; Liashenko, A.; Piskorz, P.; Komaromi, I.; Gomperts, R.; Martin, R. L.; Fox, D. J.; Keith, T.; Al-Laham, M. A.; Peng, C. Y.; Nanayakkara, A.; Gonzalez, C.; Challacombe, M.; Gill, P. M. W.; Johnson, B. G.; Chen, W.; Wong, M. W.; Andres, J. L.; Head-Gordon, M.; Replogle, E. S.; Pople, J. A. *Gaussian 98*, revision A.8; Gaussian, Inc.: Pittsburgh, PA, 1998.

(17) Ortiz, J. V. *J. Chem. Phys.* **1998**, *108*, 1008.

(18) McLean, A. D.; Chandler, G. S. *J. Chem. Phys.* **1980**, *72*, 5639.

(19) Dunning, T. H.; *J. Chem. Phys.* **1971**, *55*, 716.

(20) Chiles, R. A.; Dykstra, C. A. *J. Chem. Phys.* **1981**, *74*, 4544.

(21) Handy, N. C.; Pople, J. A.; Head-Gordon, M.; Ragavachari, K.; Trucks, G. W. *Chem. Phys. Lett.* **1989**, *164*, 185.

(22) Ortiz, J. V. *Chem. Phys. Lett.* **1998**, *296*, 494.

(23) Ortiz, J. V. *Int. J. Quantum Chem.* **1999**, *75*, 615.

(24) Ortiz, J. V. *Chem. Phys. Lett.* **1998**, *297*, 193.

(25) Schaftenaar, G. *MOLDEN 3.4*; CAOS/CAMM Center: The Netherlands, 1998.

(26) Bartlett, R. J. *Annu. Rev. Phys. Chem.* **1981**, *32*, 359.

(27) Krishnan, R.; Binkley, J. S.; Seeger, R.; Pople, J. A. *J. Chem. Phys.* **1980**, *72*, 650.

(28) Wong, M. W.; Gill, P. M. W.; Nobes, R. H.; Radom, L. *J. Phys. Chem.* **1988**, *92*, 4875.

(29) Gillies, J. Z.; Gillies, C. W.; Cotter, E. A.; Block, E.; DeOrazio, R. *J. Mol. Spectrosc.* **1996**, *180*, 139.

(30) Frisch, M. J.; Pople, J. A.; Binkley, J. S. *J. Chem. Phys.* **1984**, *80*, 3265.